A study of electronic states of trigonal and amorphous Se using ultraviolet photoemission and inverse-photoemission spectroscopies

1996 J. Phys.: Condens. Matter 8 7249

(http://iopscience.iop.org/0953-8984/8/39/004)

J. Phys.: Condens. Matter **8** (1996) 7249–7261. Printed in the UK

A study of electronic states of trigonal and amorphous Se using ultraviolet photoemission and inverse-photoemission spectroscopies

I Ono, P C Grekos†, T Kouchi, M Nakatake, M Tamura, S Hosokawa, H Namatame and M Taniguchi

Department of Materials Science, Faculty of Science, Hiroshima University, Kagamiyama 1-3, Higashi-Hiroshima 739, Japan

Received 26 March 1996, in final form 14 June 1996

Abstract. Valence-band and conduction-band densities of states (DOSs) of trigonal and amorphous Se have been investigated by *in situ* measurements of ultraviolet photoemission and inverse-photoemission spectroscopies (UPS and IPES), respectively. The IPES spectra reveal, for the first time, a measure of conduction-band DOS, while the UPS spectra are fully consistent with earlier results. From comparison between theoretical DOS and a whole spectrum for trigonal Se obtained by a connection of the UPS and IPES spectra at the Fermi level, it has been shown that the coupling strength between the hybrid 4p-like orbitals of different atoms should be increased. On the basis of a comparison between IPES and core-absorption spectra for trigonal Se, a prominent peak and weak structures in the 1–5 and 5–10 eV regions above the valence-band maximum in the IPES spectrum are experimentally assigned to the 4p-like antibonding and 4d and/or 5s states, respectively. In amorphous Se, the peak at shallower energy in the 4p-like bonding bands with two peak structures is more intense in contrast to the case of the trigonal one. Such a change is attributed to a chain structure with the dihedral angle varying randomly in sign along the chain. Increases of the bonding–antibonding splitting energy of the 4p-like bands and band-gap energy in amorphous Se are ascribed to an increase of intrachain coupling strength between the hybrid 4p-like orbitals and a simultaneous decrease of the interchain coupling strength.

1. Introduction

A crystal of trigonal Se consists of helical chains arranged in a hexagonal array oriented along the c-axis and each atom is covalently bonded to two neighbours with a bonding angle (θ) of 105° and dihedral angle (ϕ) of 102° [1, 2], as shown in figures 1(a) and (b). The dihedral angle is defined as the angle between the projection of second-neighbour bonds on a plane normal to their first neighbour. The bonding between individual chains is much weaker and is often believed to be of a weak van der Waals type. Each spiral chain has three atoms per turn with equivalent atoms on adjoining chains forming a hexagonal plane network of atoms.

Two electrons per Se atom with a valence orbital configuration of $(4s)^2(4p)^4$ fill the lowest 4s-like levels. The remaining four electrons fill the 4p-like orbitals: two of them

† Present address: Laboratory for Research on the Structure of Matter, University of Pennsylvania, 3231 Walnut Street, Philadelphia, PA 19104-6202, USA.

0953-8984/96/397249+13$19.50

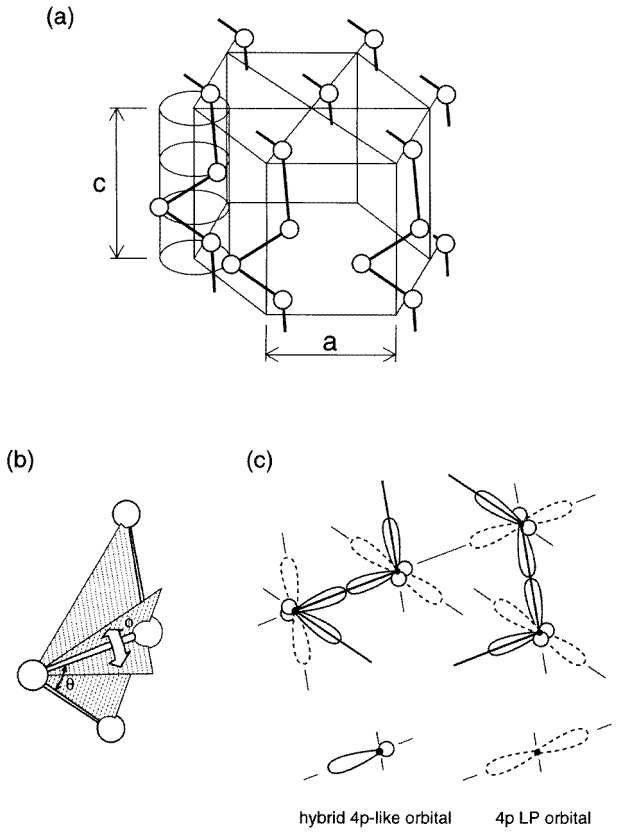

Figure 1. (*a*) Crystal structure of trigonal Se that consists of helical chains arranged in a hexagonal array oriented along the *c*-axis. The unit cell consists of three atoms in one helix. Lattice constants are $a = b = 4.355$ Å, $c = 4.949$ Å. (*b*) A part of a chain. θ and ϕ represent bonding angle (105°) and dihedral angle (102°), respectively. (*c*) Arrangement of hybrid 4p-like and LP orbitals (full and broken lines, respectively). The thick full lines represent the chain.

form covalent bonds with electrons on the nearest neighbours, while the remaining two form lone-pair (LP) states [3], as shown in figure 1(*c*).

The density of states (DOS) of trigonal Se in the valence-band region has been investigated by means of ultraviolet and x-ray photoemission spectroscopies (UPS and XPS) [4–6]. The UPS and XPS spectra exhibited a prominent peak at −2 eV, two peaks between −3.5 and −7 eV, as well as two broad peaks between −11 and −17 eV with respect to the valence-band maximum (VBM). These peaks were attributed to the LP, 4p-like bonding and 4s-like states, respectively.

The electronic band-structure calculations for trigonal Se have been performed by various approaches over the years [2]. A detailed account should include the Kohn–Rostker method [7], the tight-binding model [8–11], the pseudopotential [12], the empirical pseudopotential method (EPM) [10], the vector charge density wave model [13] as well as the self-consistent symmetrized orthogonalized-plane-wave method [14]. The valence-band DOS accomplished by the EPM was in excellent agreement with the experimental photoemission spectra [5]. A rough picture of the electronic structure of Se can be obtained by considering the strong intrachain bonding only [10]. The DOS of Se 4s bands closely

resembles a one-dimensional chain with two singularities at the band edges. Since the atomic 4s-like states are well separated from the shallower 4p-like states, it is expected that the s–p mixing will be small in the crystal. This does not contradict a bond angle of about 105° if one allows for slight mixing with 4d states as well [10].

Little comparison, however, has been made between theory and experiment for the conduction-band DOS, because direct experimental information on the unoccupied electronic states has been fairly limited so far. Specifically, the results of band-structure calculations have usually been tested by comparison to the experimental optical constants [15]. However, such comparisons are not conclusive, because several alterations in the valence and conduction bands or the transition matrix elements can produce the necessary adjustments needed to fit the experimental optical results.

Valence-band spectra for amorphous Se have been obtained by means of UPS and XPS [4–6, 16], and then, the valence-band features have been revealed to be close to those for the trigonal form. In amorphous Se, an order between chains shown in figure 1(*a*) is expected to be lost. Consequently, the condition of overlap between orbitals shown in figure 1(*c*) would be changed. The effect on electronic states caused by the loss of an order in the amorphous form has been an object of great interest.

In this paper, we present valence-band and conduction-band spectra for trigonal and amorphous Se measured by means of ultraviolet photoemission and inverse-photoemission spectroscopies (UPS and IPES). The IPES spectra reveal, for the first time, the structural features of the conduction-band DOS, in particular energy positions and widths of the 4p-like antibonding bands and higher lying 4d-like bands. We show that *in situ* measurements of UPS and IPES spectra realize a connection of these two spectra at the Fermi level (E_F) in the band gap and thus provide a whole DOS spectrum. This makes it possible to discuss the relative energy positions of the experimental DOS peaks derived from the 4s-, 4p- and 4d-like states, and to compare with the calculated DOS for the trigonal form. In addition, we compare the IPES spectrum with Se 2p and 3d core-absorption spectra to evaluate the contributions of the 4p-, 4d- and 5s-like states to the conduction-band DOS. Finally, we discuss the UPS and IPES spectra for amorphous Se in comparison with those for the trigonal one.

2. Experimental details

The UPS and IPES spectrometers employed in this study [17] are shown schematically in figure 2. The apparatus is connected with a preparation chamber and a crystal growth chamber. The UPS spectrometer consists of a He discharge lamp and a double-stage cylindrical-mirror analyser. The energy resolution was set to be 0.2 eV.

The IPES spectrometer contains an Erdman–Zipf-type electron gun with a BaO cathode mounted on the symmetry axis of an Al mirror coated with an MgF_2 film to improve reflectivity. A monoenergetic electron beam from the electron gun, which can deliver a high beam current down to low kinetic energy (for instance, 2 μA at 5 eV and 10 μA at 20 eV), was focused onto the sample. Light emitted from the sample was focused by the Al reflection mirror and detected using a bandpass photon detector [18]. Overall energy resolution of the IPES spectrometer, which depends on both the full width at half maximum of the photon detector (0.47 eV) and the energy spread of the electron beam (0.25 eV), was 0.56 eV centred at 9.43 eV [18].

Base pressures of preparation, crystal growth, UPS and IPES chambers were 2 ×

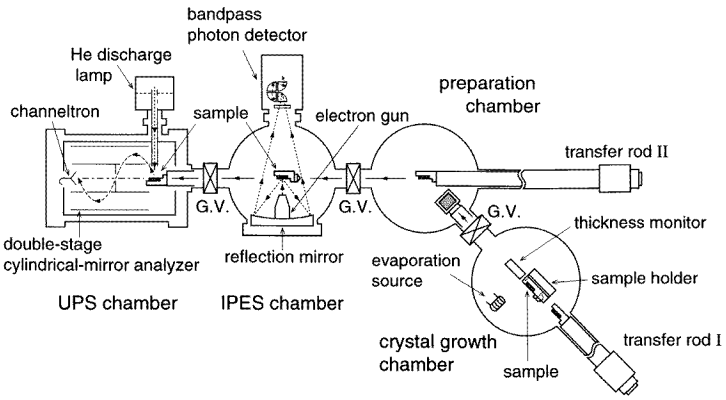

Figure 2. A schematic illustration of the apparatus used for UPS and IPES measurements. The UPS spectrometer consists of a He discharge lamp and a double-stage cylindrical-mirror analyser. The IPES spectrometer contains an Erdman–Zipf-type electron gun mounted on the symmetry axis of an Al mirror and a bandpass photon detector [18]. The crystal growth chamber contains an evaporation source of Se, a quartz thickness monitor and sample holder with a heating system. Se films are transferred *in situ* into the preparation chamber by transfer rod I and subsequently into the UPS and IPES chambers using transfer rod II.

10^{-10}, 7×10^{-10}, 8×10^{-10} and 8×10^{-10} Torr, respectively†. The working pressure of the UPS chamber under the operation of the He discharge lamp was 3×10^{-9} Torr.

The energy calibrations of the UPS and IPES apparatus were achieved experimentally using the spectra for a fresh film of polycrystalline Au evaporated on a Mo substrate. The UPS and IPES spectra were connected at the E_F by measuring these spectra *in situ* for the same sample surface. The position of the E_F in the band gap depends upon the respective samples, while the energies of the UPS and IPES spectra can be defined experimentally relative to the E_F. Therefore, the connection of both spectra at the E_F due to *in situ* measurements is inevitably important to evaluate the energy separation between peaks in the valence-band DOS and those in the conduction-band DOS.

The samples used were polycrystalline bulk and thin films of Se. The bulk sample was an undoped crystal with a trigonal form prepared by melt–quenching and further annealing at 150 °C. A clean surface was prepared *in situ* by scraping with a diamond file for UPS measurements. The resistivity of the bulk sample was of the order of MΩ, making IPES measurements difficult due to an electrostatic charging effect, although the resistivity was low enough to avoid such an effect in the present UPS measurements. To overcome such a difficulty, we prepared thin films on conductive Au substrates.

Thin films of Se were prepared *in situ* in the crystal growth chamber attached to the preparation chamber as shown in figure 2. For preparation of trigonal thin films we evaporated Se onto Au substrates kept at room temperature (RT) with a rate of 9 Å s^{-1} and total thickness of 1 μm. The sample thickness and rate of evaporation were measured by means of a quartz thickness monitor placed near the sample. The pressure under evaporation was 1×10^{-8} Torr. We further directly heated up the substrates at 105 °C for 13 min to obtain polycrystalline films with a trigonal form. Re-evaporation of deposited Se atoms was

† Although base pressures of crystal growth and IPES chambers in the measurements for bulk trigonal Se and trigonal Se films were 7×10^{-10} and 8×10^{-10} Torr, respectively, both of them for amorphous Se films were 2×10^{-10} Torr.

observed. Amorphous films were prepared by evaporating Se atoms onto Au substrates at RT with a rate of 2 Å s^{-1} until a thickness of 100 Å had been achieved. The Se films were transferred *in situ* into the preparation chamber using transfer rod I and subsequently into the UPS and IPES chambers using transfer rod II.

Crystalline and amorphous forms of bulk sample and films were checked by x-ray diffraction and Raman scattering measurements. The UPS spectrum for the bulk trigonal Se was also used as a reference in the characterization of the polycrystalline thin film of trigonal Se.

The UPS and IPES spectra of the bulk trigonal Se and trigonal and amorphous Se films were measured within one hour after the preparation, and are assumed to be reasonably

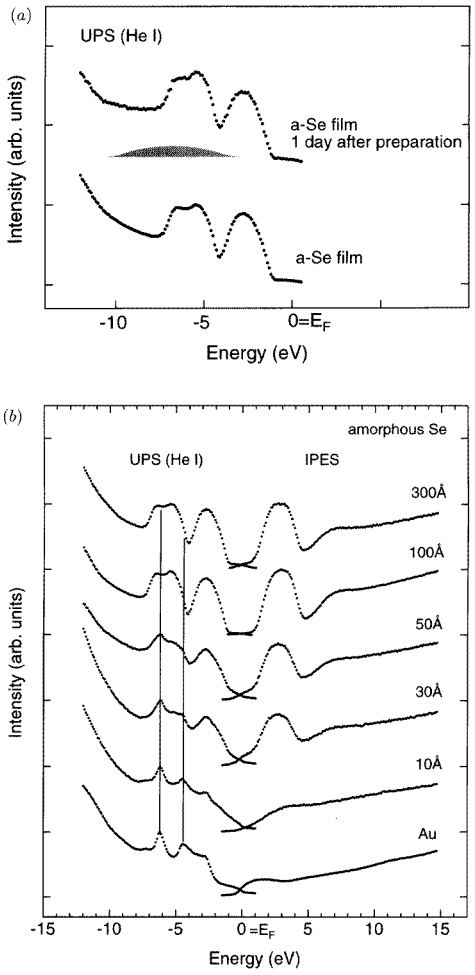

Figure 3. (*a*) UPS spectra of amorphous Se film measured at the excitation photon energy of 21.2 eV (He I). The lower spectrum is for the film just after preparation. The upper one is for the film left for one day under a vacuum level of 2×10^{-10} Torr. The shaded area shows schematically an additional broad structure due to surface contamination. (*b*) UPS (He I) and IPES spectra for amorphous Se films of 0–300 Å thickness. The energy is referred to the E_F. Vertical bars represent energy positions of structures due to the Au substrate.

free from surface contamination. Such a contamination effect was weakly observed for the sample surface left for one day under a vacuum level of 2×10^{-10} Torr in the present study and could be recognized as an additional broad structure in the UPS spectrum, as shown schematically in figure 3(*a*).

In the measurements of the UPS and IPES spectra for amorphous Se films, an attenuation of Au features was carefully checked by changing the thickness of films. UPS and IPES spectra of amorphous Se films with thickness below 50 Å exhibited structures due to the Au substrate in addition to those originated from amorphous Se. With the increase of thickness the intensity of Au features decreased, and above 100 Å in thickness the contribution from the Au substrate disappeared completely and no detectable change was observed between the spectra for films with thicknesses of 100 and 300 Å with respect to spectral shapes and peak positions as shown in figure 3(*b*). For trigonal Se films the possibility of a contribution from Au substrates was ruled out from a comparison of the UPS spectrum measured just after the re-evaporation of Se on the annealed Se film with the UPS spectrum of bulk trigonal Se, which was completely free from Au features. In general, the surface sensitivity of the IPES spectrum is better than that of the UPS spectrum. Therefore, when the UPS spectrum is free from the contribution from the Au substrate, the IPES spectrum is reasonably assumed to reflect intrinsic features of trigonal Se†.

As concerns electrostatic charging, we found no detectable effect in the UPS and IPES spectra for trigonal and amorphous Se films. Such an effect can be observed easily as an energy shift of structures in the present experiments‡.

3. Results and discussion

First, we discuss the crystallization of amorphous film using UPS spectra. In figures 4(*a*)–(*c*) we show the UPS spectra for a thin film of amorphous Se, bulk trigonal Se and a thin film of trigonal Se, respectively, measured at the excitation photon energy of 21.2 eV (He I). All energies are referred to E_F. Both spectra for (*a*) the amorphous Se film and (*b*) bulk trigonal Se are in excellent agreement with those measured previously under ultra-high vacuum below $(3–5) \times 10^{-10}$ Torr [4, 5, 16] with respect to their spectral shapes and relative peak positions.

The valence-band spectrum for the bulk trigonal Se (figure 4(*b*)) exhibits two main peaks; the LP bands around -3 eV and the 4p-like bonding bands with the well resolved two-peak structures in the energy region from -4 to -8 eV. From a comparison between the spectra for (*a*) the amorphous Se film and (*b*) bulk trigonal Se, one notices a remarkable difference in the 4p-like bonding bands. The spectrum for the amorphous sample has structures at -5.5 and -6.5 eV, and the peak at -5.5 eV carries more weight than the other, while that for bulk crystal has a major peak at -5.9 eV and a minor peak at -4.9 eV.

† Recently, we performed photoemission measurements using synchrotoron radiation at the Photon Factory in the National Laboratory for High Energy Physics (KEK-PF) for amorphous and trigonal Se films prepared by the same methods. The valence-band UPS spectrum measured at 40.8 eV was consistent with that shown in figure 5(*b*). The attenuation of Au in the films was also checked by the measurements for the Au 4f core level region.

‡ In the present IPES experiments, photon intensity is measured as a function of kinetic energy (E_k) of the electron beam (E_k = 0–20 eV). Then, the intensity of the electron beam changes depending on E_k, for example, 0 μA at $E_k = 0$ eV, 2 μA at $E_k = 5$ eV and 10 μA at $E_k = 20$ eV, during the measurement. Therefore, one can easily check experimentally whether the electrostatic charging effect is taking place or not in the second scanning of the electron beam. We have confirmed that there is no detectable charging effect in the IPES spectra of trigonal and amorphous Se films. For the UPS spectra of amorphous Se films, the absence of electrostatic charging effect has also been checked from comparison of UPS spectra for the films with thickness up to 300 Å as shown in figure 3(*b*).

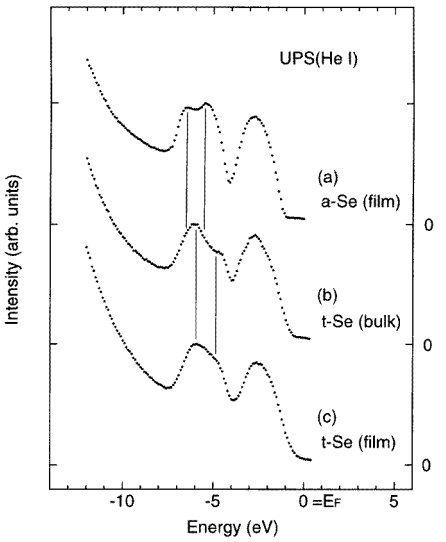

Figure 4. UPS spectra for (*a*) thin film of amorphous Se, (*b*) bulk trigonal Se and (*c*) thin film of trigonal Se, measured at the excitation photon energy of 21.2 eV (He I). All energies are referred to E_F.

One can recognized that spectrum (*c*) is similar to spectrum (*b*) with respect to their spectral features. Within the resolution of the UPS spectrometer, there is no basic difference between these two spectra. Therefore, we assume that spectrum (*c*) reflects features intrinsic to the trigonal Se.

Figure 5(*a*) shows the valence-band UPS measured at 21.2 eV (He I) and conduction-band IPES spectra for a trigonal Se film. The energy of the UPS and IPES spectra is drawn with respect to the VBM, which is determined by extrapolating the leading edge of the valence bands to the base line, after their connection at the E_F. The threshold energy of the IPES spectrum evaluated by extrapolating the leading edge is in good agreement with the band-gap energy (E_g) of 1.6 eV obtained by optical measurements [19]. The UPS spectrum measured at 40.8 eV (He II) is also shown in figure 5(*b*) (dotted curve) to demonstrate structures in the region from -10 to -16 eV. The valence-band spectra exhibit structures at -1.0, -2.0, -4.4 and -5.4 eV (vertical bars), in agreement with the results of earlier UPS and XPS measurements [4–6, 16]. On the other hand, the conduction-band spectrum shows a prominent peak at 3.4 eV and weak structures at 7.6 and 8.4 eV above the VBM (vertical bars).

Full curves in figure 5(*b*) exhibit the theoretical DOSs of trigonal Se calculated by Joannopoulos *et al* using the EPM [10]. The energy of the theoretical curves is also referred to the VBM. Calculated valence bands in the energy regions from 0 to -2.5 eV, from -2.5 to -5.5 eV and from -10 to -16 eV are derived from the LP, 4p-like bonding and 4s-like states, respectively. Peaks around -3.2 and -4.5 eV have been related to interchain and intrachain bonding states, respectively [20]. Conduction bands at 2–5 eV are due to the 4p-like antibonding states.

One can recognize that the theory describes well the features of the valence-band spectrum. In particular, with respect to the relative energy positions of DOS peaks in the valence bands, there appears to be an excellent agreement between the experiment and

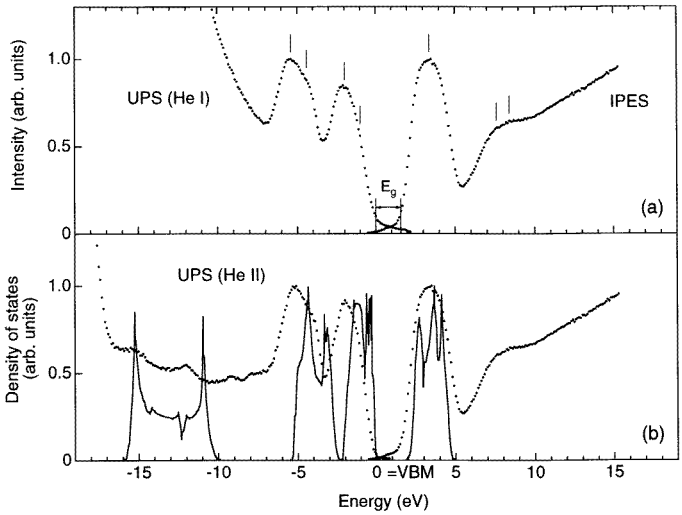

Figure 5. (*a*) Valence-band UPS and conduction-band IPES spectra for trigonal Se film measured at an excitation photon-energy of 21.2 eV (He I). The two spectra are connected at the E_F and energy is referred to the VBM. Vertical bars represent energy positions of structures. A band-gap energy (E_g) is estimated from positions of thresholds determined by extrapolating leading edges of the UPS and IPES spectra to the base line. (*b*) The calculated DOS of trigonal Se [10] (full curves). The valence-band UPS spectrum measured at 40.8 eV (He II) and the conduction-band IPES spectrum (dotted curves) are also shown for comparison between the theory and experiment.

theory. In the present results, however, all peaks of the theoretical DOS are reproduced shallower in energy than those of the experimental one. Theoretical widths of the LP and 4p-like bonding bands are narrower than that of the experimental DOS. Relative intensities of theoretical DOS peaks in the 4p-like bonding bands are also in good agreement with those in the UPS spectrum.

Although the calculation has been performed with no direct information on the experimental DOS of conduction bands, the theoretical curve reproduces fairly well the features of the conduction-band spectrum in the energy position of the 4p-like antibonding bands, and in relative intensities and energy positions of DOS peaks inside the antibonding bands. However, taking into account the features of valence bands, it appears that the theoretical estimation of the 4p-like bonding–antibonding splitting energy is smaller than that obtained in the present experiments.

From a comparison between experimental and theoretical results, we point out that the centre-of-mass energy of the LP and 4p-like bonding bands in the theoretical DOS should be placed at energies deeper by about 0.9 and 1.2 eV, respectively. Then, the bonding–antibonding splitting energy of the 4p-like bands should also be increased by about 1.2 eV. An increase of the coupling strength between the hybrid 4p-like orbitals for different atoms, which are primarily of atomic 4p nature with some 4s and 4d admixture, would increase the splitting energy and thus provide an increase of widths of the 4p-like bonding and antibonding bands.

Further, we compare the IPES spectrum with the Se $2p_{3/2}$ and 3d core-absorption spectra for trigonal Se measured by Belin *et al* [21] and Cardona *et al* [22] in figures 6(*a*) and (*b*), respectively (full curves). The IPES spectrum shown by a dotted curve in figure 6(*a*)

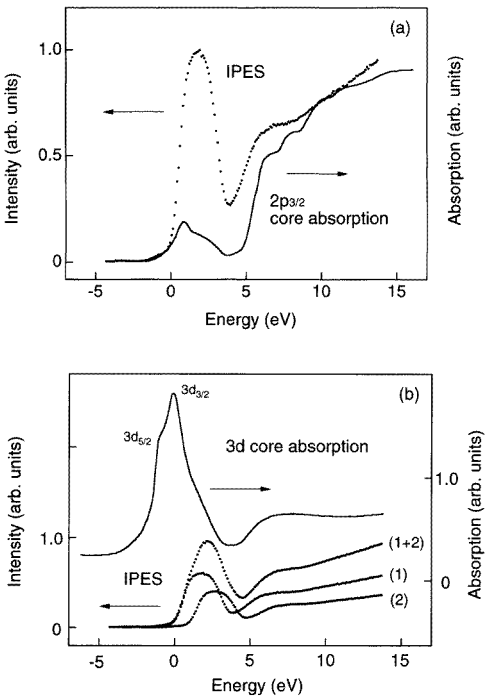

Figure 6. (*a*) The $2p_{3/2}$ core-absorption spectrum [21] (full curve) and the IPES spectrum (dotted curve) for trigonal Se. Energy is referred to the thresholds of these spectra. (*b*) The 3d core-absorption spectrum [22] (full curve) and IPES spectra (dotted curves) for trigonal Se. The dotted curve $(1 + 2)$ represents a spectrum constructed by a superposition of two experimental IPES curves (1) and (2) weighted in the ratio of 6:4 and shifted by 0.9 eV. Energy is referred to the threshold of the IPES spectrum (1).

is arranged as the threshold coincides with that of the core-absorption spectrum and energy is referred to these thresholds. The 3d core-absorption spectrum in figure 6(*b*) consists of $3d_{5/2}$ and $3d_{3/2}$ components. The threshold of the IPES spectrum (1) is adjusted to the $3d_{5/2}$ core-absorption threshold (56.2 eV), estimated from the sum of the band-gap energy (1.6 eV) and the Se $3d_{5/2}$ core-level energy with respect to the VBM (54.6 eV). Curve $(1 + 2)$ represents a spectrum constructed by a superposition of two experimental IPES curves (1) and (2) weighted in the ratio of 6:4 statistical weight of the initial Se $3d_{5/2}$ and $3d_{3/2}$ core states and shifted by the spin–orbit splitting energy of 0.9 eV. The horizontal axis of figure 6(*b*) is redrawn with respect to the threshold of the IPES spectrum (1).

The core-absorption spectra provide information on the conduction-band DOS including the selection rule of angular momentum on optical transitions. Therefore, we can derive contributions of each orbital component to the conduction-band DOS, from a comparison between the IPES and core-absorption spectra.

One notices that the shape of the Se 2p and 3d core-absorption spectra are quite different to each other due to the selection rule for the excitations. The Se 2p core spectrum in figure 6(*a*) exhibits a weak and broad peak in the energy region from 0 to 4 eV, and structures with a steep threshold near 4 eV in agreement with the feature of IPES spectrum in the energy region from 4 to 10 eV.

On the other hand, the Se 3d core spectrum in figure 6(*b*) exhibits doublet structures

separated by about 0.9 eV in the energy region from −2 to 1 eV, and also weak structures above 5 eV. The prominent doublet structures on the lower energy region would be most reasonably be understood as associated with the Se $3d_{5/2}$ and $3d_{3/2}$ core-exciton excitation, in analogy with the core-excitation of trigonal Te [23]. The features above 5 eV correspond well to those in the IPES (1 + 2) spectrum.

From the remarkable contrast between the Se 2p and 3d core-absorption spectra, we find experimentally that the prominent structure in the 0–4 eV region in the IPES spectrum consists mainly of the 4p-like states in agreement with the results of band-structure calculations [10], and weak structures in the energy region above 4 eV are mainly made up of the 4d and/or 5s states.

Here, we also compare the present results for trigonal Se with those for trigonal Te obtained by Taniguchi *et al* [23]. The valence-band UPS and conduction-band IPES spectra for trigonal Se and Te exhibit similar features with respect to the shape and energy positions of structures. All the LP, 5p-like bonding and 5s-like bands are observed to be in a deeper energy region in comparison with the theoretical DOSs calculated by Joannopoulos *et al* [10]. In addition, the spectral widths of the LP and 5p-like bonding bands are narrower than the theoretical ones. However, there are some differences between the spectra for trigonal Se and Te. The energy position of the main peak in the IPES spectrum coincides with that in the theoretical DOS, though the main peak is observed at higher energy in the IPES spectrum for trigonal Te.

Next, we move to discussions on the UPS and IPES spectra for amorphous Se. In figure 7 we show valence-band UPS (He I) and conduction-band IPES spectra for amorphous and trigonal Se films. Energies are drawn with respect to E_F. The spectra for amorphous Se exhibit structures at −6.5, −5.5, −2.8 and −2.0 eV in valence bands, and at 2.1, 3.0, 3.5, 7.4, 8.2 and 10.4 eV in conduction bands, while those for trigonal Se exhibit at −5.9, −4.9, −2.5 and −1.5 eV in valence bands, and at 2.9, 7.1 and 7.9 eV in conduction bands. These results are summarized in table 1.

From comparison between the spectra for amorphous and trigonal Se, one can recognize

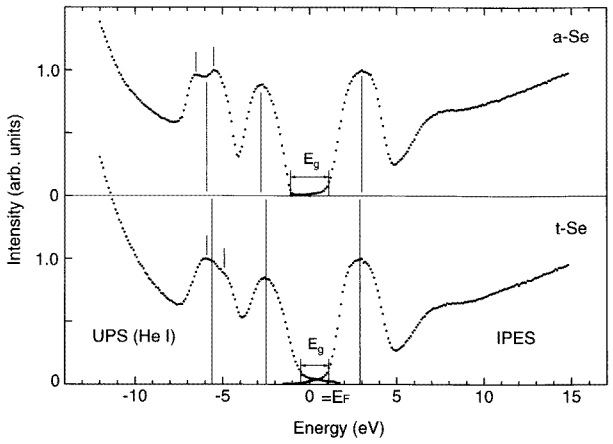

Figure 7. Valence-band UPS (He I) and conduction-band IPES spectra for amorphous and trigonal Se films. The UPS and IPES spectra are connected at the E_F. All energies are referred to E_F. E_g represents band-gap energy. Long vertical bars exhibit coarse positions of centre-of-mass energy for the respective bands.

Table 1. Energy positions of structures in valence-band UPS (He I) and conduction-band IPES spectra for amorphous (a-) and trigonal (t-) Se. Energies are in eV and are referred to E_F.

	UPS					IPES				
a-Se	−6.5	−5.5	−2.8	−2.0	2.1	3.0	3.5	7.4	8.2	10.4
t-Se	−5.9	−4.9	−2.5	−1.5	—	2.9	—	7.1	7.9	—

that the band structure of amorphous Se is similar to those of trigonal Se with respect to the 4p-like bonding, LP, 4p-like antibonding and 4d and/or 5s bands. However, the heights of the two peaks in the 4p-like bonding bands of trigonal Se (vertical bars) are reversed in the amorphous phase. Long vertical bars exhibit coarse positions of the centre-of-mass energy for respective bands. We find that the amount of the bonding–antibonding splitting energy of the 4p-like bands in amorphous Se increase roughly by 0.3–0.4 eV to that in the trigonal one. The 4p-like bonding and LP bands of amorphous Se shift by about 0.3 eV to the deeper energy side, while the 4p-like antibonding bands stay at almost the same energy position. The band-gap energy for amorphous Se is evaluated to be 2.2 eV, which is larger than 1.6 eV for the trigonal one. In addition, the width of the LP bands from -4 to -1 eV in amorphous Se is narrower than that from -4 to -0.5 eV in the trigonal one.

Bullett *et al* calculated DOSs for several structures of Se by means of a local orbital method [24]. Figure 8(*a*) shows the resulting DOS for trigonal Se, consisting of the 4p-like bonding, LP and 4p-like antibonding bands. We find a close agreement with EPM results [10] and experiments [4–6], although there are some differences in the energy positions and widths of the calculated bands. Figure 8(*b*) exhibits the DOS for the chain structure with an alternating sign and constant magnitude of dihedral angle ($\phi = \pm 102^\circ$) along the chain. The alternating dihedral angle is characteristic of the puckered Se_8 rings in the monoclinic form. One notices that the 4p-like bonding bands acquire a two-peak structure in figure 8(*b*), where the peak on the shallower energy side carries more weight in contrast to the trigonal case (*a*). The calculated DOS (*b*) is in good agreement with the experimental spectrum for monoclinic Se [6]. Figure 8(*c*) displays the DOS for a model in which the dihedral angle varies randomly in sign along the chain with the absolute value of the constant angle of 102°. The calculated DOS is again found to show a reverse of the heights of two peaks in close agreement with the experimental results of the amorphous form in figure 7.

From dissolution of amorphous Se in CS_2 [25], Raman scattering [26], x-ray photoemission [6] and x-ray and neutron diffraction [27, 28] measurements, it is well known that the Se_8 rings are very few in number and thus negligible in amorphous Se, and that amorphous Se consists of a chain-like structure with nearly unchanged geometry from trigonal Se, but with random orientations. Therefore, we can reasonably assume that the reversal of the two peak heights in the 4p-like bonding bands of amorphous Se is mainly due to the chain structure with random sign of dihedral angle, within a framework of the model by Bullett *et al* [24].

The increase of the bonding–antibonding splitting energy of the 4p-like bands in amorphous Se is understood by taking into account an increase of the coupling between the hybrid 4p-like orbitals on different atoms as a result of the decrease of the nearest-neighbour distance. The densities of amorphous and trigonal Se are 4.3 and 4.8 g cm^{-3}, respectively [29]. This suggests that the interchain coupling in amorphous Se would be weaker than that in trigonal one. Theoretical analysis of the character of interchain forces in trigonal Se shows that the decrease of the interchain coupling strength results in the increase of a covalent character within chains [30]. Geometrical packing of the possible chains in amorphous Se

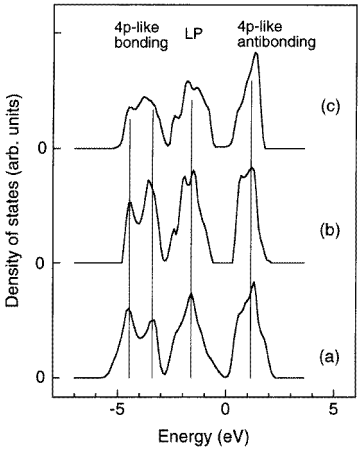

Figure 8. Calculated DOSs for Se with several structures [24]. (*a*) DOS for trigonal Se composed of helical chains of atoms. (*b*) DOS for a chain structure with an alternating dihedral angle $\phi = \pm 102^\circ$ along the chain. The alternating dihedral angle is characteristic of the puckered Se_8 ring in the monoclinic form. (*c*) The DOS for a model in which the dihedral angle has a random sign along the chain with the absolute value of the constant angle of 102°.

is such that all interchain couplings are weak [30]. This is supported by results of extended x-ray absorption fine-structure measurements [31], which indicate shorter nearest neighbours and a longer interchain distance in amorphous Se compared to trigonal Se.

The increase of the band-gap energy in amorphous Se can be attributed to both the increase of the 4p-like bonding–antibonding splitting energy due to the increase of the intrachain coupling strength and the decrease of the width of the LP bands as a result of the decrease of the coupling strength in the interchain interaction. We find from figure 1(c) that the trigonal Se forms such that each LP orbital overlaps with the primarily 4s-like orbitals and the back lobes of the hybrid 4p-like orbitals on atoms of adjacent chains, providing a sizable dispersion in the LP bands. Therefore, the narrowing of width of the LP bands is reasonably expected in amorphous Se, since the chains are more isolated in amorphous Se than in trigonal Se.

4. Conclusion

Thin films of Se with trigonal and amorphous form were prepared and *in situ* measurements of UPS and IPES spectra were performed. From a comparison between the theoretical DOS and experimental whole DOS spectrum for trigonal Se, it was shown that the coupling strength between the hybrid 4p-like orbitals on different atoms should be increased.

Comparison between the IPES and core-absorption spectra revealed that the prominent structure and weak structures in the 1–5 and 5–10 eV regions in the IPES spectrum consist mainly of 4p-like antibonding and 4d and/or 5s states, respectively.

The heights of the two peaks in the 4p-like bonding bands in the UPS spectrum for amorphous Se are reversed in comparison with those for trigonal Se. The chain structure with the dihedral angle varying randomly in sign along the chain is assumed to be the dominant source for such a reversal. The bonding–antibonding splitting energy of the 4p-like bands and band-gap energy of amorphous Se are larger than those of trigonal Se. These

effects are interpreted by taking into account an increase of the intrachain coupling strength and a simultaneous decrease of the interchain coupling strength.

Acknowledgments

The authors are grateful to Professors K Murase and K Nagata for their fruitful discussions and Dr O Matsuda for the Raman scattering measurements. We would like to thank C Ueda and T Ohba for their assistance in measurements. One of us (IO) was supported by Fellowships of the Japan Society for the Promotion of Science for Japanese Junior Scientists, and PCG would like to express his sincere acknowledgments for the financial support from the Japanese–German Center in Berlin (JGCB) and the Japanese Ministry of Foreign Affairs. This work is partly supported by the Grant-in-Aid for Science Research from the Ministry of Education, Science and Culture, Japan, Iketani Science and Technology Foundation, The Ogasawara Foundation for the Promotion of Science and Technology, The Murata Science Foundation, Shimazu Science Foundation and Tokuyama Science Foundation.

References

[1] Wyckoff R 1963 *Crystal Structures* 2nd edn, vol 1 (New York: Interscience) p 36
[2] Joannopoulos J D 1979 *Physics of Selenium and Tellurium* (Berlin: Springer)
[3] Kastner M 1972 *Phys. Rev. Lett.* **28** 355
[4] Shevchik N J, Cardona M and Tejeda J 1973 *Phys. Rev.* B **8** 2833
[5] Shevchik N J, Tejeda J, Cardona M and Langer D W 1973 *Solid State Commun.* **12** 1285
[6] Takahashi T, Murano K, Nagata K and Miyamoto Y 1983 *Phys. Rev.* B **28** 4893
[7] Treusch J and Sandrock R 1966 *Phys. Stat. Sol.* **16** 487
[8] Reitz J R 1957 *Phys. Rev.* **105** 1233
[9] Olechna D J and Knox R S 1965 *Phys. Rev.* A **140** 986
[10] Joannopoulos J D, Sclüter M and Cohen M L 1975 *Phys. Rev.* B **11** 2186
[11] Nizzoli F 1977 *Nuovo Cimento* B **39** 135
[12] Sandrock R 1968 *Phys. Rev.* **169** 642
[13] Oka T and Fukutome H 1988 *Prog. Theor. Phys.* **79** 608
[14] Krusius P, von Boehm J and Stubb T 1975 *Phys. Stat. Sol.* b **67** 551
[15] Tutihasi S and Chen I 1967 *Phys. Rev.* **158** 623
[16] Takahashi T, Ohno K and Harada Y 1980 *Phys. Rev.* B **21** 3399
[17] Yokoyama M, Nishihara K, Mimura K, Hari Y, Taniguchi M, Ueda Y and Fujisawa M 1993 *Rev. Sci. Instrum.* **64** 87
[18] Ueda Y, Nishihara K, Mimura K, Hari Y, Taniguchi M and Fujisawa M 1993 *Nucl. Instrum. Methods* A **330** 140
[19] Stuke J 1970 *J. Non-Cryst. Solids* **4** 1
[20] Schlüter M, Joannopoulos J D and Cohen M L 1974 *Phys. Rev. Lett.* **33** 89
[21] Belin E, Senemaud C and Bonnelle C 1978 *J. Non-Cryst. Solids* **27** 119
[22] Cardona M, Gudat W, Sonntag B and Yu P 1970 *Proc. 10th Int. Conf. on the Physics of Semiconductors* p 209
[23] Taniguchi M, Tamura M, Hari Y, Sato H, Nakatake M, Namatame H, Hosokawa S and Ueda Y 1994 *J. Phys.: Condens. Matter* **6** 5181
[24] Bullett D W 1975 *J. Phys.: Condens. Matter* **8** L377
[25] Lucovsky G 1979 *The Physics of Selenium and Tellurium* ed E Gerlach and P Grosse (New York: Springer) p 178
[26] Nagata K 1995 Private communication
[27] Corb B W, Wei W D and Averbach B L 1982 *J. Non-Cryst. Solids* **53** 29
[28] Henninger E H, Buschert R C and Heaton L 1967 *J. Chem. Phys.* **46** 586
[29] 1982 *McGraw-Hill Encyclopedia of Science and Technology* 5th edn, vol 12 (New York: McGraw-Hill) p 252
[30] Martin R M, Lucovsky G and Helliwell K 1976 *Phys. Rev.* B **13** 1383
[31] Tamura K, Hosokawa S, Endo H, Yamasaki S and Oyanagi H 1986 *J. Phys. Soc. Japan* **55** 528